

Irradiation-induced changes of martensitic transformation temperatures in a TiNiNb shape memory alloy

H.Q. Mo^{a,b}, X.T. Zu^{a,*}, Y. Huo^c

^a Department of Applied Physics, University of Electronic Science and Technology of China, Chengdu 610054, PR China

^b Department of Material Forming and Controlling Engineering, Sichuan University, Chengdu 610065, PR China

^c Department of Mechanics, Fudan University, Shanghai 200433, PR China

Received 11 July 2004; received in revised form 12 September 2004; accepted 24 September 2004

Abstract

Effects of electron irradiations on the transition behavior of 1123 K annealed Ti₄₄Ni₄₇Nb₉ shape memory alloy specimens were studied. The transformation temperatures and the latent heat of phase transformation were measured by differential scanning calorimeter (DSC). The microstructure changes were determined by XRD and TEM. The 1.7 MeV electron irradiation increases the martensitic transformation start temperature, finish temperature, austenite transformation start, finish temperature by ~20 K. The XRD and TEM observation showed that the volume fraction of β-Nb precipitate increased after electron irradiation, which contributed to the observed changes of the transformation temperatures.

© 2004 Elsevier B.V. All rights reserved.

PACS: 73.61.At; 74.25.Fy; 81.40.Wx

Keywords: TiNiNb shape memory alloys; Electron irradiation effects; Transmission electron microscopy; Differential scanning calorimeter; Martensitic transformation

1. Introduction

Ternary TiNiNb shape memory alloys (SMAs) are distinct from TiNi binary SMAs for its wide phase transformation temperature hysteresis [1–7]. The constitutional phases of TiNiNb SMA are β-Nb particles and TiNi matrix. During deformation at low temperature, β-Nb particles and the matrix are deformed simultaneously. Upon heating the matrix to its original shape, the soft β-Nb particles prohibit the recovery of the matrix. Thus the expanded joining, fastening and sealing device can be shipped and stored at ambient temperature in the martensitic state, i.e., in the as-

expanded shape. Therefore, this ternary alloy has great potential applications as mechanical components in the field of fission and fusion engineering and space technology [1,5]. There are some reports on the irradiation effect of TiNi(Cu) SMAs under neutron, proton, electron and heavy-ion irradiation [6–18]. As far as the authors' knowledge is concerned, the irradiation effect of TiNiNb SMAs has not been reported.

The martensitic transformation characteristics in SMAs are very sensitive to various physical factors (such as precipitates, dislocations, point defects and chemical composition) so that the radiation effect of SMAs is perplexing. The neutron irradiation up to about 1 dpa was found to produce a strong decrease of the transition temperatures [6,12]. This decrease is believed to be due to the pronounced

* Corresponding author. Tel.: +86 28 83201939; fax: +86 28 83201939.
E-mail address: xiaotaozu@yahoo.com (X.T. Zu).

chemical disordering of the crystal lattice [6,13]. The electron irradiation to about $1.7 \times 10^{21} \text{ e/m}^2$ (10^{-5} dpa) led to a higher equilibrium temperature and martensitic stabilization, had little effect on reverse martensitic transformation temperature in a ternary TiNiCu shape memory alloy [14]. It was found in high voltage electron microscopy that the electron irradiation (2 MeV) decreased reverse martensitic transformation temperature above a dose of $7 \times 10^{24} \text{ e/m}^2$ [10].

In the present work, the irradiation effect on the martensitic transformation characteristics and microstructures in a near-equiatomic TiNiNb SMA have been stud-

ied by means of 1.7 MeV electron electrostatic accelerator, differential scanning calorimeter (DSC), X-ray diffraction (XRD) and transmission electron microscope (TEM).

2. Experimental

Ti₄₄Ni₄₇Nb₉ SMA samples with a thickness of 1 mm, provided by the Institute of Metal Research of the Chinese Academy of Sciences, were annealed at 1123 K for 1 h in an evacuated silica tube and then cooled in the air. After the

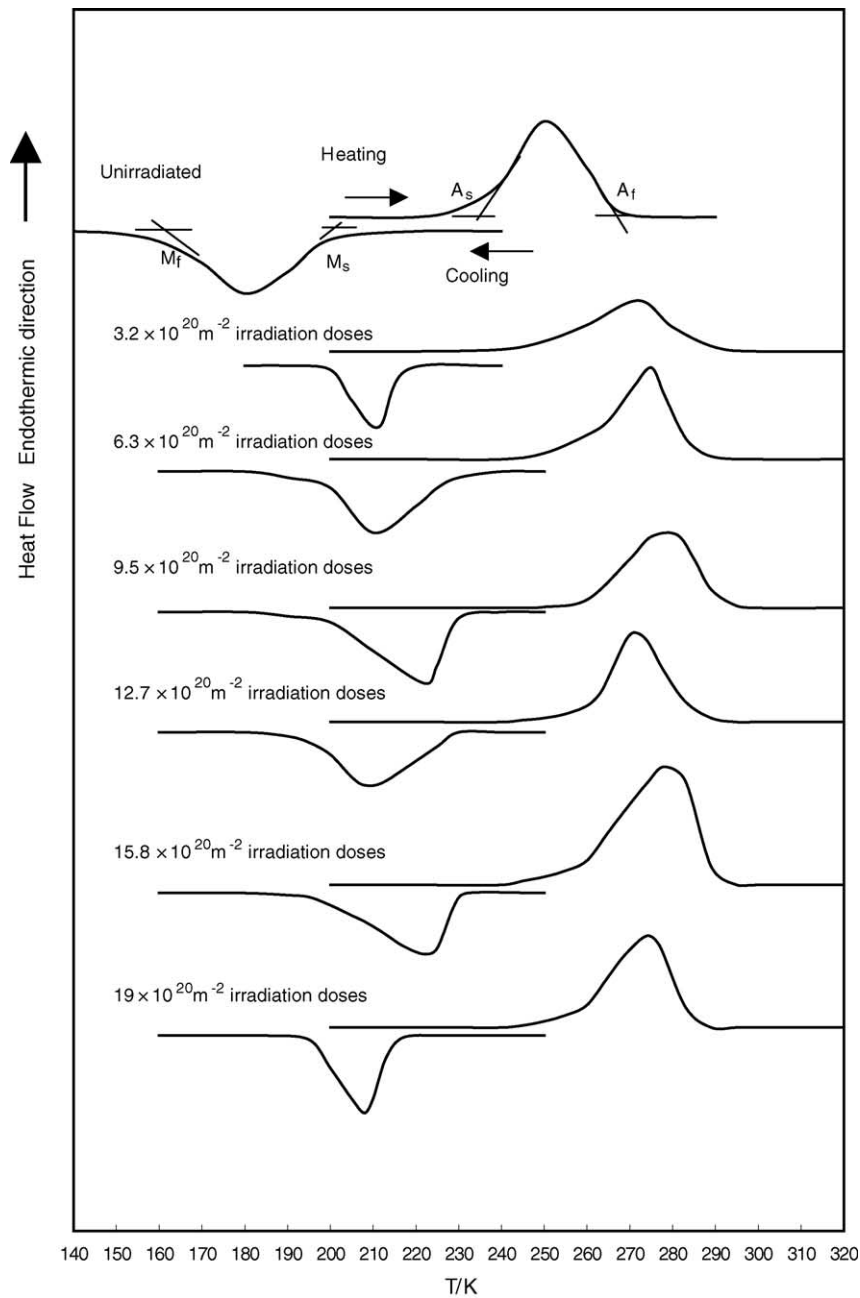


Fig. 1. DSC curves of the electron irradiated and unirradiated TiNiNb samples.

heat treatment, the samples were then irradiated to the electron dose ($E = 1.7 \text{ MeV}$) of 3.2, 6.3, 9.5, 12.7, 15.8 and $19.0 (\times 10^{20} \text{ m}^{-2})$ at the dose rate of $4.4 \times 10^{16} \text{ m}^{-2} \text{ s}^{-1}$ in air in the Electron Electrostatic Accelerator of the Key Laboratory for Radiation Physics and Technology of Education Ministry of China located in Chengdu. The temperature of the samples during the irradiation was controlled by circulating water and was maintained at about 298 K monitored by a thermocouple, well above A_f , A_s , M_s and M_f (shown in Fig. 1, M_s , M_f , and A_s , A_f is the martensitic transformation start, finish temperature, austenite transformation start, finish temperature, respectively). Thus, the samples have been kept in the austenite phase state during the electron irradiation.

The irradiated samples were placed at room temperature for about 30 days. Then, the transformation temperatures were measured by DSC between 100 and 400 K at a rate of 10 K min^{-1} . TEM analysis was performed by JEM 200 CX at the University of Electronic Science and Technology of China. The structures of samples were analyzed by X-ray diffraction (XRD) with an X-ray diffractometer type D/max-1400 pc Rigaku, Japan with Cu $K\alpha$ radiation ($\lambda = 1.5405 \text{ \AA}$)

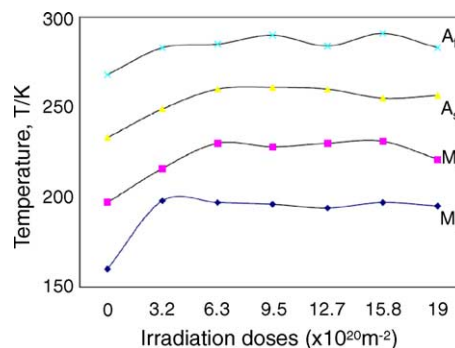


Fig. 2. Changes of transformation temperatures with the dose of electron irradiation in TiNiNb SMA samples.

by scanning in the $2\theta = 10\text{--}100^\circ$ range with 0.02° steps.

3. Results and discussion

DSC curves in Fig. 1 showed the transformation characteristic of the electron irradiated and unirradiated TiNiNb

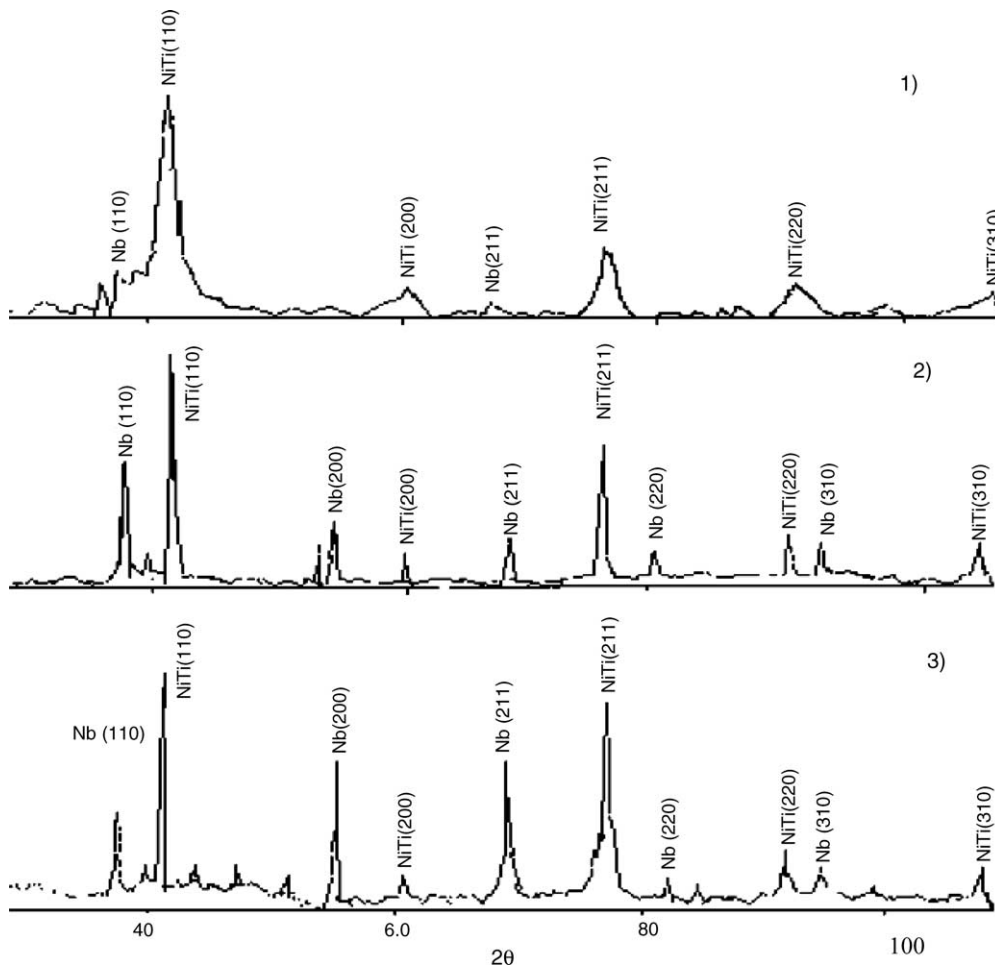


Fig. 3. The X-ray diffraction patterns of TiNiNb SMAs showing the β -Nb phase precipitated after electron irradiation: (1) unirradiated; (2) 1.7 MeV electron irradiation to a dose of $3.2 \times 10^{20} \text{ m}^{-2}$; (3) 1.7 MeV electron irradiation to a dose of $12.7 \times 10^{20} \text{ m}^{-2}$.

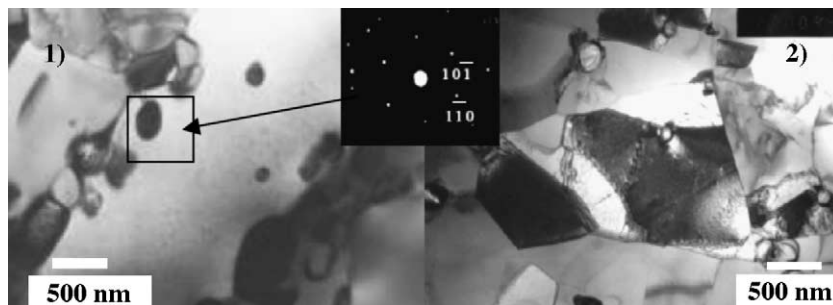


Fig. 4. Bright field TEM image of the TiNiNb SMA samples and selected area electron diffraction pattern (the insert, responding to β -Nb phase taken from rectangle area) showing that the β -Nb phase precipitated after electron irradiation: (1) after irradiation (at a dose of $19.0 \times 10^{20} \text{ m}^{-2}$); (2) before irradiation.

samples. Changes of transformation temperatures with the dose of electron irradiation in TiNiNb SMA samples are shown in Fig. 2. XRD results of the samples, which were unirradiated and irradiated at a dose of 3.2×10^{20} and $12.7 \times 10^{20} \text{ m}^{-2}$, is shown in Fig. 3. Bright field TEM image of an irradiated (at a dose of $19.0 \times 10^{20} \text{ m}^{-2}$) and unirradiated sample and selected area electron diffraction pattern (the insert) at room temperature is shown in Fig. 4.

From Fig. 2, it is obvious that all transformation temperatures of the TiNiNb SMA samples were increased quickly by ~ 20 K after irradiation with 1.7 MeV electron to a dose of $3.2 \times 10^{20} \text{ m}^{-2}$ and then kept stable almost up to $19 \times 10^{20} \text{ m}^{-2}$. The XRD results showed that the diffraction peaks of β -Nb phase rose after electron irradiation (such as Nb(1 1 0), Nb(2 0 0), Nb(2 1 1) and Nb(3 1 0) peak), as shown in Fig. 3. β -Nb precipitates were observed in the sample electron irradiated at a dose of $19 \times 10^{20} \text{ m}^{-2}$ by TEM observation in Fig. 4. The average volume fraction of β -Nb precipitate was calculated by counting the numbers of the particles in more than three different TEM pictures. The thickness of sample thin area was estimated to be 100 Å. The volume fraction increased from 4.2×10^{-13} to $8.1 \times 10^{-13} \text{ m}^{-3}$ after electron irradiation. Thus, the electron irradiation-induced β -Nb phase precipitation.

This is different from the results of electron irradiated TiNiCu and TiNi SMAs. For TiNiCu SMAs an increase of the transition temperature A_s was observed, but the electron irradiation had a slight effect on M_f , and no detectable effect on M_s [14]. They are assigned to the effect of the driving force of martensite nucleation and the stored elastic energy of martensite after the electron irradiation from a thermodynamical analysis [15]. The 1.7 MeV electron irradiation decreases the martensitic transformation start temperature M_s by 46 K to a dose of $17.4 \times 10^{20} \text{ m}^{-2}$ in a Ti–50.6 at.% Ni SMA and the other transformation temperatures had a slight changes [16]. It was believed that some point defects produced by electron irradiation migrate to the stressed borders of the Ti_3Ni_4 precipitates modifying the local atomic configuration, and relaxing the elastic energy of stress fields around the Ti_3Ni_4 precipitates and this was the cause of the observed change of the transformation characteristics of the electron irradiated TiNi SMAs. The neutron irradiation with a dose of $(3\text{--}4) \times 10^{22} \text{ m}^{-2}$ was found to produce a strong decrease of

the transition temperature M_s , M_f , A_s , A_f , which is assigned to a decrease in the degree of long-range order in the lattice caused by neutron irradiation [12].

In TiNiNb SMAs, it is obvious that the electron irradiation-induced an appearance of β -Nb precipitates (Figs. 3 and 4) and led an increase of all transformation temperatures (M_s , M_f , and A_s , A_f). The electron irradiation produces point defects (Frenkel pairs) and enhances atom diffusion [14], which induced an appearance of precipitates in TiNiNb alloy samples.

4. Conclusions

The 1.7 MeV electron irradiation increases the martensitic transformation start temperature, finish temperature, austenite transformation start, finish temperature by ~ 20 K. The XRD and TEM observation showed that β -Nb precipitates increased after electron irradiation, which contributed to the observed changes of the transformation temperatures.

Acknowledgments

This study was supported financially by the National Natural Science Foundation of China (10175042) and the Foundation of National Key Laboratory for Nuclear Fuel and Materials.

References

- [1] K. Otsuka, C.M. Wayman, *Shape Memory Materials*, Cambridge University Press, 1998, pp. 76–77.
- [2] L.C. Zhao, T.W. Duerig, S. Just, et al., *Scripta Metall. Mater.* 24 (1990) 221–226.
- [3] M. Piao, S. Miyazaki, K. Otsuka, et al., *Mater. Trans. JIM* 33 (1992) 337–345.
- [4] M. Piao, S. Miyazaki, K. Otsuka, *Mater. Trans. JIM* 33 (1992) 346–353.
- [5] T. Hoshiya, H. Sekino, Y. Matsui, F. Sakurai, K. Enami, *J. Nucl. Mater.* 233–237 (1996) 599.
- [6] T. Hoshiya, S. Den, H. Ito, S. Takamura, Y. Ichihashi, *J. Jpn. Inst. Met.* 55 (1991) 1054.

- [7] A. Barbu, A. Dunlop, A.H. Duparc, G. Jaskierowicz, N. Lorenzelli, *Nucl. Instr. Meth. B* 145 (1998) 354.
- [8] J. Cheng, A.J. Ardell, *Nucl. Instr. Meth. B* 44 (1990) 336.
- [9] Y. Matsukawa, S. Ohnuki, *J. Nucl. Mater.* 239 (1996) 261.
- [10] H. Mori, H. Fujita, *Jpn. J. Appl. Phys.* 21 (1982) 494.
- [11] S. Watanbe, T. Koike, T. Suda, S. Ohnuki, H. Takahashi, N.Q. Lam, *Phil. Mag. Lett.* 81 (2001) 789.
- [12] R.F. Konopleva, I.V. Nazarkin, V.L. Solovei, V.A. Chekanov, S.P. Belyaev, A.E. Volkov, A.I. Razov, *Phys. Solid State* 40 (1998) 1550.
- [13] S.F. Dubinin, S.G. Teploukho, V.D. Parkhomenko, *Fiz. Met. Met-alloved.* 82 (1996) 297.
- [14] X.T. Zu, L.M. Wang, Y. Huo, L.B. Lin, Z.G. Wang, *Appl. Phys. Lett.* 80 (1) (2002) 31.
- [15] X.T. Zu, C.F. Zhang, S. Zhu, Y. Huo, Z.G. Wang, L.M. Wang, *Mater. Lett.* 57 (13–14) (2003) 2099–2103.
- [16] X.T. Zu, L.B. Lin, Z.G. Wang, S. Zhu, L.P. You, L.M. Wang, Y. Huo, *J. Alloys Comp.* 351 (1–2) (2003) 87–90.
- [17] Z.G. Wang, X.T. Zu, L.J. Liu, S. Zhu, Y. Huo, L.B. Lin, X.D. Feng, L.M. Wang, *Nucl. Instr. Meth. B* 211 (2) (2003) 239–243.
- [18] X.T. Zu, S. Zhu, X. Xiang, L.P. You, Y. Huo, L.M. Wang, *Mater. Sci. Eng. A* 363 (1–2) (2003) 352–355.